Mathematical Geology, Vol. 36, No. 1, January 2004 (© 2004)

Space–Time Mathematical Framework for Sedimentary Geology[1]

Jean-Laurent Mallet[2]

Interpolating physical properties in the subsurface is a recurrent problem in geology. In sedimentary geology, the geometry of the layers is generally known with a precision much superior to that which one can reasonably expect for the properties. The geometry of the layers is affected by folding and faulting since the time of deposition, whereas the distribution of properties is, to a certain extent, determined at the time of deposition. As a consequence, it may be wise to model first the geometry of the layers and then, "simplify the geologic equation" by removing the influence of that geometry. Inspired from the work of H. E. Wheeler on "Time-Stratigraphy," we define, mathematically, a new space where all horizons are horizontal planes and where faults, if any, have disappeared. We surmise that this new space, however approximative, is better to model physical properties of the subsurface whatever the subsequent interpolation method used. The proposed mathematical framework also provides solutions to complex problems such as determination of strains resulting from tectonic events and up-scaling of permeabilities on structured and unstructured 3D grids.

KEY WORDS: property modeling, upscaling, stratigraphy, strain tensor.

INTRODUCTION

The interpolation of properties of the subsurface by geostatistical methods makes intensive use of distances between data locations and locations where the interpolation is performed (e.g., see Chiles and Delfiner, 1999; Deutsch and Journel, 1998; Goovaerts, 1997; Journal and Huijbregt, 1978; Mallet, 2002; Matheron, 1968). This raises the problem of *how* these distances should be computed. In the case where the geological structures in the subsurface are not faulted and correspond to horizontal layers, the best is to use an Euclidean coordinate system (x, y, z) with (x, y) being the horizontal coordinates and z the vertical axis. However, if the geological structures are folded, intuition suggests that a curvilinear coordinate system (u, v, t) with (u, v) axes parallel to the horizons and the t-axis orthogonal

[1]Received 1 May 2003; accepted 30 July 2003.

[2]Gocad Research Group, Ecole Nationale Supérieure de Géologie, BP 40, 54501 Vandoeuvre-lès-Nancy, France; e-mail: jean-laurent.mallet@ensg.inpl-nancy.fr

to the layers, would be more appropriate to compute geodesic distances. On the basis of these observations, we propose a Geo-Chronological model of the subsurface which can be seen as a mathematical formulation of the Time-Stratigraphy concept introduced by H. E. Wheeler (1958).

There are many examples in physics where choosing an appropriate curvilinear coordinate system reduces the complexity of problems. For example:

- the equations of flow through porous media are greatly simplified with a 3D curvilinear coordinate system (u, v, t) with (u, v) defining the isopressure surfaces and the t axis aligned with streamlines (e.g., see Mallet, 1971; Thiele and others, 1996);
- the propagation of seismic front waves (surfaces) in the subsurface is simplified if one chooses to use a 3D curvilinear coordinate system (u, v, t) where (u, v) match the seismic front wave and t corresponds to the ray paths (e.g., see Cerveny, 1985; Hubral and Kery, 1980; Mallet, 2002);
- the equations describing the deformation of terrains around a tunnel are simplified if a 3D cylindrical curvilinear system with axis aligned with the tunnel is retained (e.g., see Sokolnikoff, 1956; Timoshenko and Goodier, 1970);
- we should also mention the critical role played by 4D curvilinear coordinate systems in the theory of general relativity (Edington, 1923; Einstein, 1920).

As shown in Figure 1(A), the first generation of flow simulators used in reservoir engineering was based on a decomposition of the subsurface into a set of adjacent hexahedral cells whose edges never cross the horizons and the faults

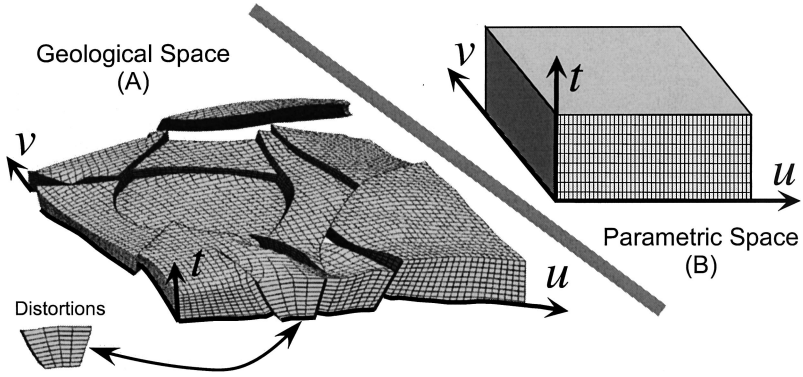

Figure 1. Example of decomposition of a reservoir into a set of hexahedral adjacent 3D cells adapted to the specific needs of a flow simulator. The edges of these cells never cross the horizons nor the faults and are aligned to constitute a 3D curvilinear coordinate system (u, v, t). There are distortions of the lengths of horizontal edges between the top and bottom cells of the reservoir.

(Aziz and Settari, 1979). These cells are aligned to generate a "stratigraphic grid" whose edges induce a curvilinear coordinate system (u, v, t) with t being oriented in the vertical direction and the (u, v) axes being parallel to the horizons (Mallet, 2002). Each point in the subsurface has an image in the (u, v, t) parametric domain and the images of the nodes of the stratigraphic grid in this parametric space constitute a regular rectilinear grid where the horizons are horizontal and are not faulted (see Fig. 1(B)). A current practice in geostatistics consists in using the parametric domain (u, v, t) so defined to compute Euclidean distances whose images in the geological domain are curvilinear distances (e.g, see Mallet, 2002). Such curvilinear coordinates account for the shape of the horizons which themselves control geological continuity. There are however two drawbacks to this approach:

- First, distortions of horizontal distances cannot be avoided when the faults are oblique relative to the horizons. For example, as shown in Figure 1(A), a pair of faults having a "V shape" in the vertical direction may generate large distortions of horizontal cell sizes from the top to bottom of a reservoir. In such a case, distances in the parametric space are irrelevant.
- Next, as shown in Figure 8, a new generation of flow simulators is using unstructured grids based on a decomposition of the subsurface into polyhedric cells which can no longer be used to compute curvilinear distances.

A new methodology for parametrization of the subsurface is proposed which avoids the previous drawbacks while providing a method to populate the cells of unstructured grids with geostatistical, structural distance-based, estimates. As a byproduct, the strain tensor of terrains can be computed everywhere in the subsurface and a new way to implement upscaling techniques is proposed.

It is important to note that the purpose of this article is to define the theoretical basis and properties of such a modeling approach, not to provide practical implementation techniques. However, hints leading to such implementations are given.

GEOCHRON MODEL

In his pioneering paper, H. E. Wheeler (1958) presented, for the first time, the concept of "*Time-Stratigraphy*." His approach was based on the initial premise that stratigraphic units can be defined in a 3D space consisting of "*two lateral space* (geographical) *dimensions and a vertical time* (chronological) *dimension*." The "Geo-Chronological model" proposed in this section and abbreviated "GeoChron model," can be seen as a mathematical formulation of the concepts introduced by Wheeler.

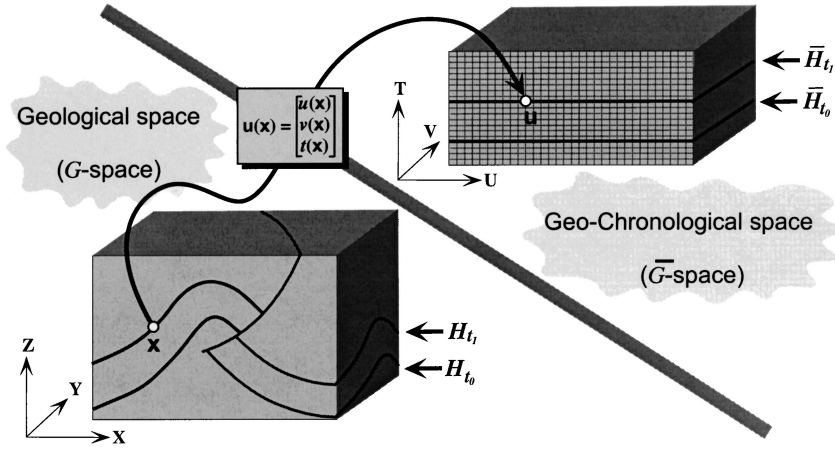

Figure 2. Geological space (abbreviated G-space) and Geo-Chronological space (abbreviated $\bar{G}$-space). Note that the image $\bar{H}_t$ in the $\bar{G}$-space of any horizon H_t of the G-space is always a horizontal plane. Note also that the transformation $\mathbf{u}(\mathbf{x})$ can (theoretically) be defined independently of any grid covering the G-space.

G-Space, Horizons and Geological Time

As depicted in Figure 2, let G be a bounded volume of interest in the 3D geological space as observed today. G may be cut by a series of faults and unconformities which, in turn, may induce a partition of G into a finite set of parts called "fault blocks." By definition, we propose to call "Geological-space" or, more simply, G-space, the 3D space where the region of interest G defined above is embedded. Any point belonging to the G-space is denoted $\mathbf{x}$ such that

$$\mathbf{x} = x \cdot \mathbf{X} + y \cdot \mathbf{Y} + z \cdot \mathbf{Z} \tag{1}$$

where $(\mathbf{X}, \mathbf{Y}, \mathbf{Z})$ is a given right-handed orthogonal frame of unit vectors. For the sake of conciseness, we will also denote by $\mathbf{x}$ the column matrix whose elements are the components (x, y, z) of $\mathbf{x}$ in the $(\mathbf{X}, \mathbf{Y}, \mathbf{Z})$ frame:

$$\mathbf{x} = [x, y, z]^t \tag{2}$$

The terrains contained in the G-space are assumed to have been generated as follows:

1. At geological time t, particles of sediment are deposited on a part $\bar{H}_t$ of a horizontal plane representing the surface of the earth (or the bottom of the sea). Note that the horizontal bar above H_t is proposed as a reminder of the fact that $\bar{H}_t$ is (a part of) a horizontal plane.

2. Because of tectonic events occurring during geological time $\tau > t$, the originally flat horizontal plane $\overline{H}_t$ is transformed into a surface H_t, observable today and called a "horizon," which may be both faulted and folded. Note that, with such a definition, a horizon H_t is actually a "isochronal" horizon which may not be coincident with a traditional "geophysical" horizon extracted from a seismic cube.

Using seismic and well data and geomodeling techniques (e.g., Mallet, 2002), it is possible to actually observe and build numerical representations of the finite series of horizons $\{H_{t_0}, H_{t_1}, \cdots, H_{t_n}\}$ sorted by chronological order:

$$t_0 < t_1 < \cdots < t_n \tag{3}$$

It is important to note that the geological time t so defined should not be confused with the "age" of the terrains:

$$t_i < t_j \Longleftrightarrow H_{t_i} \text{ is older than } H_{t_j}$$

Note also that, provided they honor the inequalities (3), the geological times $\{t_0, t_1, \cdots\}$ associated with the horizons need not be known with precision and can even be chosen arbitrarily.

Paleogeographic Coordinates

At any geological time t, we are interested in building an image (map) of the surface of the earth showing the distribution of the particles of sediment in the region of interest. The mathematical model presented in this article is based on two assumptions:

- any particle of sediment initially deposited at geological time $(t - \Delta t)$ then eroded before being redeposited at time t is considered as a new particle;
- the properties of the particles, as they are observed today, strongly depend on their location at geological time t of deposition. In other words, tectonic movements (faulting and folding) affect locations but have no or few effects on the particles properties.

As a consequence of the second hypothesis above, reconstructing images of the location of particles at their geological time of deposition is critical for a geologically consistent interpolation of the present day distribution of physical properties in the G-space.

As suggested in Figure 3, consider a geostationary satellite equipped with a camera shooting vertically towards the surface of the earth in the region under study. This camera is defined by a right-handed frame of three orthogonal unit

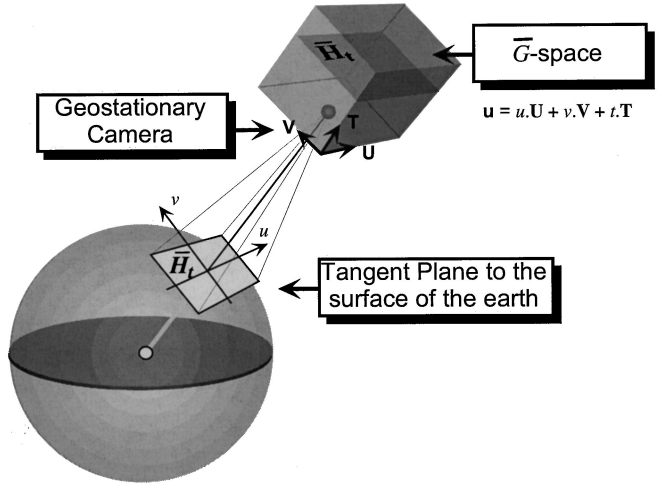

Figure 3. $\bar{G}$-space viewed as a continuous chronological stacking of images $\{\bar{H}_t\}$ of the surface of the earth taken from a geostationary camera throughout geological time t.

vectors (**U**, **V**, **T**) where **T** is orthogonal to the surface of the earth and oriented upward. These three vectors define the edges of a box where the images taken by the camera are assumed to be stacked in chronological order during geological time. For coherence with the geological processes, the camera is geostationary in the sense that its (**U**, **V**, **T**) axis are "attached" to the tectonic plate containing the domain of interest.

Let $\bar{H}_t$ be the horizontal plane orthogonal to the vector **T** and corresponding to the surface of the earth at geological time t. Note that $\bar{H}_t$ is parallel to the pair of orthogonal unit vectors (**U**, **V**) which can thus be used as a frame for $\bar{H}_t$. As a consequence, for any given reference point $\mathbf{p}_0$ belonging to $\bar{H}_t$, the pair of vectors (**U**, **V**) induces a coordinate system (u, v) on $\bar{H}_t$ such that:

$$\mathbf{p} \in \bar{H}_t \Longleftrightarrow \exists (u, v) \in I\!R^2 : \mathbf{p} = \mathbf{p}_0 + u \cdot \mathbf{U} + v \cdot \mathbf{V}$$

At geological time t, the (u, v) coordinate system so defined can thus be used to locate any particle being deposited on $\bar{H}_t$. For this reason, we propose to call (u, v) the "paleogeographic coordinates" system of $\bar{H}_t$.

$\bar{G}$-Space

As shown in Figure 3, imagine that we stack, "continuously" throughout geological time, all the pictures $\{\bar{H}_{t_0}, \bar{H}_{t_1}, \cdots\}$ in the 3D box defined by the vectors (**U**, **V**, **T**) attached to the camera in such a way that:

- each picture $\bar{H}_t$ is orthogonal to the vector **T** and intersects this geological time axis at abscissa t;
- the paleogeographic coordinates (u, v) attached to each picture $\bar{H}_t$ are parallel to the (**U**, **V**) vectors.

We propose to call "Geo-Chronological space" or, more simply, "$\bar{G}$-space" the (**U**, **V**, **T**) parametric space identified to the box where the images are stacked. The image of any particle of sediment deposited at geological time t at the paleogeographic location (u, v) is thus located at a point **u** in this box in such a way that:

$$\mathbf{u} = u \cdot \mathbf{U} + v \cdot \mathbf{V} + t \cdot \mathbf{T} \tag{4}$$

For the sake of conciseness, we will also denote by **u** the column matrix whose elements are the components (u, v, t) of **u** in the (**U**, **V**, **T**) frame:

$$\mathbf{u} = [u, v, t]^t \tag{5}$$

Any particle of sediment observed today, at location **x** in the G-space, was deposited at some location (u, v) on a plane $\bar{H}_t$ and can thus be characterized in a unique way by its coordinates (u, v, t) in the $\bar{G}$-space. As a consequence, as shown in Figure 2 there exist three functions $u(\mathbf{x})$, $v(\mathbf{x})$, and $t(\mathbf{x})$ transforming any point **x** of the G-space into a point $(u(\mathbf{x}), v(\mathbf{x}), t(\mathbf{x}))$ of the $\bar{G}$-space. The vectorial function $\mathbf{u}(\mathbf{x})$ defining that transformation is called a "$\bar{G}$-parametrization" of the G-space:

$$\mathbf{x} = \begin{bmatrix} x \\ y \\ z \end{bmatrix} \in G \xrightarrow{\mathbf{u}} \mathbf{u}(\mathbf{x}) = \begin{bmatrix} u(\mathbf{x}) \\ v(\mathbf{x}) \\ t(\mathbf{x}) \end{bmatrix} \in \bar{G} \tag{6}$$

Note that there is an infinity of possible $\bar{G}$-parametrizations, each, say $\mathbf{u}'(\mathbf{x}) = [u'(\mathbf{x}), v'(\mathbf{x}), t'(\mathbf{x})]^t$, being deduced from any other, say $\mathbf{u}(\mathbf{x}) = [u(\mathbf{x}), v(\mathbf{x}), t(\mathbf{x})]^t$, by rescaling the geological time t and rotating and translating the paleogeographic coordinates (u, v) as follows:

$$\underbrace{\begin{bmatrix} u'(\mathbf{x}) \\ v'(\mathbf{x}) \\ t'(\mathbf{x}) \end{bmatrix}}_{\mathbf{u}'(\mathbf{x})} = \begin{bmatrix} \begin{bmatrix} \cos(\alpha) & -\sin(\alpha) \\ \sin(\alpha) & \cos(\alpha) \end{bmatrix} \cdot \begin{bmatrix} u(\mathbf{x}) \\ v(\mathbf{x}) \end{bmatrix} \\ F(t(\mathbf{x})) \end{bmatrix} + \begin{bmatrix} \Delta_u \\ \Delta_v \\ \Delta_t \end{bmatrix} \tag{7}$$

In such a reparametrization, $F(t)$ is assumed to be an arbitrary monotonic increasing function, α is an arbitrary rotation angle while Δ_u, Δ_v, and Δ_t are arbitrary constants.

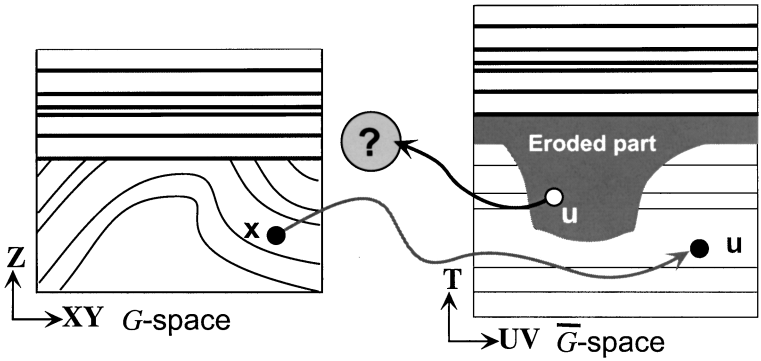

Figure 4. Vertical cross section showing an eroded zone in the $\bar{G}$-space which does not have any counterpart in the G-space.

Parametric Representation of the G-Space

Referring to Figure 4, one can observe that:

- any point $\mathbf{x}$ in the G-space has an image $\mathbf{u}(\mathbf{x})$ in the $\bar{G}$-space;
- due to erosion, there are points in the $\bar{G}$-space which have no counterpart in the present time G-space.

To account for such erosions, introduce the notion of "parametric domain" $\bar{G}_0$ as the subset of the $\bar{G}$-space whose points are images of points of the G-space:

$$\mathbf{u}^* \in \bar{G}_0 \Longleftrightarrow \exists \mathbf{x}^\star \in G \ : \ \mathbf{u}(\mathbf{x}^\star) = \mathbf{u}^\star \in \bar{G} \tag{8}$$

In other words, $\bar{G}_0$ corresponds, in the $\bar{G}$-space, to terrains which have been preserved throughout geological time. According to Wheeler's terminology, in Time-Sedimentology the parametric domain $\bar{G}_0$ so defined is called "*Holostrome*" (*holo* = complete plus *strom* = layer).

It is now possible to define as follows a function $\mathbf{x}(\mathbf{u})$ on the parametric domain $\bar{G}_0$:

$$\mathbf{u}^\star \in \bar{G}_0 \quad \xrightarrow{\mathbf{x}} \quad \mathbf{x}(\mathbf{u}^\star) \in G \ : \ \mathbf{u}(\mathbf{x}(\mathbf{u}^\star)) = \mathbf{u}^* \tag{9}$$

The function $\mathbf{x}(\mathbf{u})$ so defined on $\bar{G}_0$ is called the "parametric representation" of the G-space associated with the $\bar{G}$-parametrization $\mathbf{u}(\mathbf{x})$. Most of the time, for the sake of simplicity it is useful to express this function as an explicit function of the components of $\mathbf{u}$ and this is why we will also use the following equivalent

notation:

$$\mathbf{u} \equiv [u, v, t]^t \Longrightarrow \mathbf{x}(u, v, t) \equiv \mathbf{x}(\mathbf{u}) \tag{10}$$

As Figure 5 shows, note that:

- if t is fixed while (u, v) vary, then $\mathbf{x}(u, v, t)$ moves on the horizon H_t;
- if (v, t) are fixed while u varies, then $\mathbf{x}(u, v, t)$ moves on a curve called a u-line belonging to the horizon H_t;
- if (u, t) are fixed while v varies, then $\mathbf{x}(u, v, t)$ moves on a curve called a v-line belonging to the horizon H_t;
- if (u, v) are fixed while t varies, then $\mathbf{x}(u, v, t)$ moves on a curve called a t-line cutting the stack of horizons.

Note also that the image of a t-line in the $\bar{G}$-space is a vertical line corresponding to particles which where deposited at the same paleo-geographical coordinates (u, v) across geological time. For this reason, most of the time in the following, the name "t-line" is replaced by the name "Iso-Paleo-Geographic" line, abbreviated "*IPG*-line," which carries more explicitly the physical nature of these lines.

Notion of G-Frame $(\mathbf{x}_u, \mathbf{x}_v, \mathbf{x}_t)$

As shown in Figure 5, at each point $\mathbf{x} = \mathbf{x}(u, v, t)$ in the G-space, the parametric representation $\mathbf{x}(u, v, t)$ induces a curvilinear coordinate system consisting

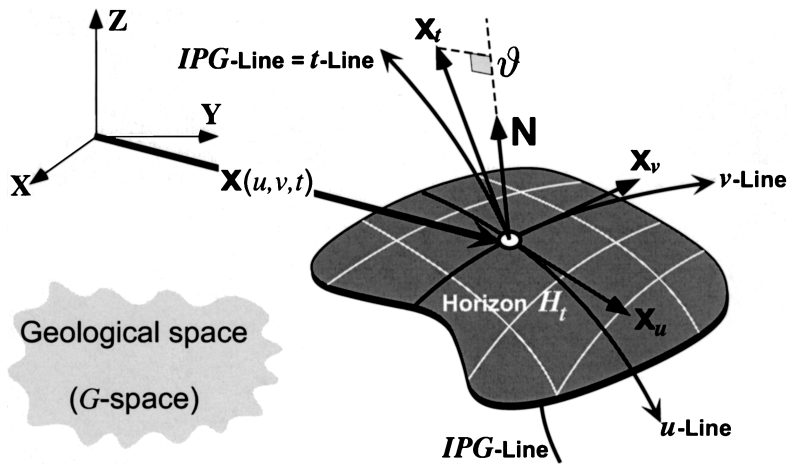

Figure 5. The parametric representation $\mathbf{x}(u, v, t)$ induces a curvilinear coordinate system in the G-space associated with a G-frame $(\mathbf{x}_u, \mathbf{x}_v, \mathbf{x}_t)$. Note that $(\mathbf{x}_u, \mathbf{x}_v)$ are tangent to the horizon H_t while the sedimentation velocity ϑ is equal to the length of the orthogonal projection of the vector $\mathbf{x}_t$ onto the direction $\mathbf{N}$ orthogonal to H_t.

of a u-line, a v-line, and a t-line and the three tangent vectors $\mathbf{x}_u(\mathbf{x})$, $\mathbf{x}_v(\mathbf{x})$ and $\mathbf{x}_t(\mathbf{x})$ defined as:

$$\begin{aligned}
\mathbf{x}_u(\mathbf{x}) &= \left.\frac{\partial \mathbf{x}(u, v(\mathbf{x}), t(\mathbf{x}))}{\partial u}\right|_{u=u(\mathbf{x})} \\
\mathbf{x}_v(\mathbf{x}) &= \left.\frac{\partial \mathbf{x}(u(\mathbf{x}), v, t(\mathbf{x}))}{\partial v}\right|_{v=v(\mathbf{x})} \\
\mathbf{x}_t(\mathbf{x}) &= \left.\frac{\partial \mathbf{x}(u(\mathbf{x}), v(\mathbf{x}), t)}{\partial t}\right|_{t=t(\mathbf{x})}
\end{aligned} \tag{11}$$

We propose to call the vectors $(\mathbf{x}_u, \mathbf{x}_v, \mathbf{x}_t)$ so defined the (local) "G-frame" associated with the G-parametrization $\mathbf{u}(\mathbf{x})$.

In the following, we will show how the gradients of the components $u(\mathbf{x})$, $v(\mathbf{x})$, and $t(\mathbf{x})$ of vector $\mathbf{u}(\mathbf{x})$ can be used to compute the vectors $(\mathbf{x}_u, \mathbf{x}_v, \mathbf{x}_t)$ at any point $\mathbf{x}$ in the G-space. For this purpose let us consider, as an example, the vector $\mathbf{x}_t(\mathbf{x})$ and let $(u^\star, v^\star)$ be the values of $u(\mathbf{x})$ and $v(\mathbf{x})$ at location $\mathbf{x}$. At this location, the t-line and its associated tangent vector $\mathbf{x}_t(\mathbf{x})$ are parallel to the intersection of the tangent planes to the isovalue surfaces $u(\mathbf{x}) = u^\star$ and $v(\mathbf{x}) = v^\star$ whose normal vectors are themselves parallel to $\mathbf{grad}\, u(\mathbf{x})$ and $\mathbf{grad}\, v(\mathbf{x})$, respectively. As a consequence, if we note $(\mathbf{a} \times \mathbf{b})$ the cross product of two vectors $\mathbf{a}$ and $\mathbf{b}$, then we can write

$$\mathbf{x}_t(\mathbf{x}) = \varepsilon \cdot ||\mathbf{x}_t(\mathbf{x})|| \cdot \frac{\mathbf{grad}\, u(\mathbf{x}) \times \mathbf{grad}\, v(\mathbf{x})}{||\mathbf{grad}\, u(\mathbf{x}) \times \mathbf{grad}\, v(\mathbf{x})||} \tag{12}$$

where $\varepsilon = \pm 1$ depends on the orientation of the t-line. Now, let us try to determine the modulus $||\mathbf{x}_t(\mathbf{x})||$. First, observe that the derivative of the curvilinear abscissa s along the t-line passing by $\mathbf{x}$ is such that:

$$||\mathbf{x}_t(\mathbf{x})|| = \left|\frac{ds}{dt}\right| \tag{13}$$

Next, let us consider the unit vector $\mathbf{d}(\mathbf{x}) = \mathbf{x}_t(\mathbf{x})/||\mathbf{x}_t(\mathbf{x})||$ tangent to the t-line passing by $\mathbf{x}$. It is well known that the derivative of $t(\mathbf{x})$ relative to the displacement s in the direction of $\mathbf{d}(\mathbf{x})$ is equal to the following dot product:

$$\frac{dt}{ds} = \mathbf{d}(\mathbf{x}) \cdot \mathbf{grad}\, t(\mathbf{x}) \tag{14}$$

As a consequence, from (12) and (14), it can be deduced that:

$$\frac{dt}{ds} = \varepsilon \cdot \frac{\mathbf{grad}\, u(\mathbf{x}) \times \mathbf{grad}\, v(\mathbf{x})}{||\mathbf{grad}\, u(\mathbf{x}) \times \mathbf{grad}\, v(\mathbf{x})||} \cdot \mathbf{grad}\, t(\mathbf{x}) \tag{15}$$

According to (12), (13), and (15), we conclude that the vector $\mathbf{x}_t(\mathbf{x})$ defined by the third Equation (11) can be deduced as follows from the gradients of the functions $u(\mathbf{x})$, $v(\mathbf{x})$, and $t(\mathbf{x})$:

$$\mathbf{x}_t(\mathbf{x}) = \varepsilon \cdot \frac{\mathbf{grad}\, u(\mathbf{x}) \times \mathbf{grad}\, v(\mathbf{x})}{(\mathbf{grad}\, u(\mathbf{x}) \times \mathbf{grad}\, v(\mathbf{x})) \cdot \mathbf{grad}\, t(\mathbf{x})} \tag{16}$$

For consistency, $\mathbf{x}_t(\mathbf{x})$ should be oriented in the same direction as $\mathbf{grad}\, t(\mathbf{x})$; in other words, ε should be chosen in such a way that:

$$\mathbf{x}_t(\mathbf{x}) \cdot \mathbf{grad}\, t(\mathbf{x}) \; > \; 0 \tag{17}$$

As a direct consequence of Equation (16) we conclude that ε must be taken equal to $+1$.

Using a circular permutation of (u, v, t), one can use exactly the same derivation to find the expressions for the vectors $\mathbf{x}_u(\mathbf{x})$ and $\mathbf{x}_v(\mathbf{x})$. Finally:

$$\left| \begin{array}{l} \mathbf{x}_u(\mathbf{x}) = \dfrac{\mathbf{grad}\, v(\mathbf{x}) \times \mathbf{grad}\, t(\mathbf{x})}{(\mathbf{grad}\, u(\mathbf{x}) \times \mathbf{grad}\, v(\mathbf{x})) \cdot \mathbf{grad}\, t(\mathbf{x})} \\ \mathbf{x}_v(\mathbf{x}) = \dfrac{\mathbf{grad}\, t(\mathbf{x}) \times \mathbf{grad}\, u(\mathbf{x})}{(\mathbf{grad}\, u(\mathbf{x}) \times \mathbf{grad}\, v(\mathbf{x})) \cdot \mathbf{grad}\, t(\mathbf{x})} \\ \mathbf{x}_t(\mathbf{x}) = \dfrac{\mathbf{grad}\, u(\mathbf{x}) \times \mathbf{grad}\, v(\mathbf{x})}{(\mathbf{grad}\, u(\mathbf{x}) \times \mathbf{grad}\, v(\mathbf{x})) \cdot \mathbf{grad}\, t(\mathbf{x})} \end{array} \right. \tag{18}$$

In differential geometry, the (twice covariant) "metric tensor" $g(\mathbf{x})$ associated with a frame $(\mathbf{x}_u, \mathbf{x}_v, \mathbf{x}_t)$ is traditionally defined as follows at any point $\mathbf{x}$ in the G-space:

$$g(\mathbf{x}) = \begin{bmatrix} ||\mathbf{x}_u||^2 & \mathbf{x}_u \cdot \mathbf{x}_v & \mathbf{x}_u \cdot \mathbf{x}_t \\ \mathbf{x}_v \cdot \mathbf{x}_u & ||\mathbf{x}_v||^2 & \mathbf{x}_v \cdot \mathbf{x}_t \\ \mathbf{x}_t \cdot \mathbf{x}_u & \mathbf{x}_t \cdot \mathbf{x}_v & ||\mathbf{x}_t||^2 \end{bmatrix} \tag{19}$$

It can be shown (e.g., see Mallet, 2002; Sedov, 1975; Sokolnikoff, 1964) that this metric tensor characterizes metric properties such as lengths, angles, areas, and volumes in the neighborhood of $\mathbf{x}$ and we will see, later in this article, how it can be used to characterize the deformation of the terrains between geological time of deposition and present time. According to Equations (18), it is interesting to note that $(\mathbf{grad}\, u, \mathbf{grad}\, v, \mathbf{grad}\, t)$ is the (contravariant) dual frame of $(\mathbf{x}_u, \mathbf{x}_v, \mathbf{x}_t)$ from which it can be deduced that the inverse of $g(\mathbf{x})$ can be expressed as follows (e.g.,

see Sedov, 1975, p. 61):

$$g^{-1}(\mathbf{x}) = \begin{bmatrix} ||\mathbf{grad}\, u||^2 & \mathbf{grad}\, u \cdot \mathbf{grad}\, v & \mathbf{grad}\, u \cdot \mathbf{grad}\, t \\ \mathbf{grad}\, v \cdot \mathbf{grad}\, u & ||\mathbf{grad}\, v||^2 & \mathbf{grad}\, v \cdot \mathbf{grad}\, t \\ \mathbf{grad}\, t \cdot \mathbf{grad}\, u & \mathbf{grad}\, t \cdot \mathbf{grad}\, v & ||\mathbf{grad}\, t||^2 \end{bmatrix} \tag{20}$$

The determinant of $g^{-1}(\mathbf{x})$ can also be expressed as follows in function of the gradients of $u(\mathbf{x})$, $v(\mathbf{x})$, and $t(\mathbf{x})$:

$$\det\left(g^{-1}(\mathbf{x})\right) = \{(\mathbf{grad}\, u(\mathbf{x}) \times \mathbf{grad}\, v(\mathbf{x})) \cdot \mathbf{grad}\, t(\mathbf{x})\}^2 \tag{21}$$

Unit Normal Vector N(x)

Let $\mathbf{N}(\mathbf{x})$ be the unit normal vector orthogonal to the horizon H_t passing by the point $\mathbf{x}$. This vector is parallel to $\mathbf{grad}\, t(\mathbf{x})$ and should thus be defined as follows to point towards the younger terrains:

$$\mathbf{N}(\mathbf{x}) = \frac{\mathbf{grad}\, t(\mathbf{x})}{||\mathbf{grad}\, t(\mathbf{x})||} \tag{22}$$

As shown in Figure 5, the vectors $(\mathbf{x}_u(\mathbf{x}), \mathbf{x}_v(\mathbf{x}))$ are tangent to the horizon H_t passing by the point $\mathbf{x}$ and are thus orthogonal to $\mathbf{N}(\mathbf{x})$. In differential geometry (DoCarmo, 1976), it is common practice to define $\mathbf{N}(\mathbf{x})$ as follows:

$$\mathbf{N}(\mathbf{x}) = \frac{\mathbf{x}_u(\mathbf{x}) \times \mathbf{x}_v(\mathbf{x})}{||\mathbf{x}_u(\mathbf{x}) \times \mathbf{x}_v(\mathbf{x})||} \tag{23}$$

The two formulae (22) and (23), however, may result in opposite orientations for $\mathbf{N}(\mathbf{x})$. To avoid such inconsistency, it is mandatory to choose the pair of functions $(u(\mathbf{x}), v(\mathbf{x}))$ in such a way that:

$$(\mathbf{x}_u(\mathbf{x}) \times \mathbf{x}_v(\mathbf{x})) \cdot \mathbf{grad}\, t(\mathbf{x}) > 0 \quad \forall\, \mathbf{x} \in G \tag{24}$$

Using the formula

$$(\mathbf{a} \times \mathbf{b}) \times (\mathbf{b} \times \mathbf{c}) = -\{(\mathbf{a} \times \mathbf{c}) \cdot \mathbf{b}\} \cdot \mathbf{b}$$

it can be shown that condition (24) is equivalent to:

$$(\mathbf{grad}\, u(\mathbf{x}) \times \mathbf{grad} v(\mathbf{x})) \cdot \mathbf{grad}\, t(\mathbf{x}) > 0 \quad \forall\, \mathbf{x} \in G \tag{25}$$

In the case where this consistency condition is not honored, one must change the sign of one of the two first components, $u(\mathbf{x})$ or $v(\mathbf{x})$, of $\mathbf{u}(\mathbf{x})$. In the rest of this article, the condition (25) is assumed honored.

Image of the Frame $(\mathbf{x}_u, \mathbf{x}_v, \mathbf{x}_t)$ in the $\bar{G}$-Space

According to the definition (11), the vector $\mathbf{x}_u(\mathbf{x})$ is such that:

$$\mathbf{x}_u(\mathbf{x}) = \lim_{\Delta u \to 0} \frac{\mathbf{x}(u(\mathbf{x}) + \Delta u,\, v(\mathbf{x}),\, t(\mathbf{x})) - \mathbf{x}(u(\mathbf{x}),\, v(\mathbf{x}),\, t(\mathbf{x}))}{\Delta u}$$

This implies that the image of $\mathbf{x}_u(\mathbf{x})$ in the $\bar{G}$-space is thus a vector $\bar{\mathbf{x}}_u(\mathbf{x})$ such that:

$$\begin{aligned}\bar{\mathbf{x}}_u(\mathbf{x}) &= \lim_{\Delta u \to 0} \frac{\begin{bmatrix} u(\mathbf{x}) + \Delta u \\ v(\mathbf{x}) \\ t(\mathbf{x}) \end{bmatrix} - \begin{bmatrix} u(\mathbf{x}) \\ v(\mathbf{x}) \\ t(\mathbf{x}) \end{bmatrix}}{\Delta u} \\ &= \lim_{\Delta u \to 0} \frac{1}{\Delta u} \cdot \begin{bmatrix} \Delta u \\ 0 \\ 0 \end{bmatrix} = \begin{bmatrix} 1 \\ 0 \\ 0 \end{bmatrix} = \mathbf{U}\end{aligned}$$

In other words, the image of $\mathbf{x}_u(\mathbf{x})$ in the $\bar{G}$-space is identical to the unit vector $\mathbf{U}$ of the frame $(\mathbf{U}, \mathbf{V}, \mathbf{T})$ associated with our geostationary camera. The images of $\mathbf{x}_v(\mathbf{x})$ and $\mathbf{x}_t(\mathbf{x})$ in the $\bar{G}$-space can be obtained in a similar way, thus:

$$\forall\, \mathbf{x} \in G : \left| \begin{aligned} \bar{\mathbf{x}}_u(\mathbf{x}) &= \mathbf{U} \\ \bar{\mathbf{x}}_v(\mathbf{x}) &= \mathbf{V} \\ \bar{\mathbf{x}}_t(\mathbf{x}) &= \mathbf{T} \end{aligned} \right. \tag{26}$$

As a consequence, any infinitely small vector $d\mathbf{W}(\mathbf{x})$ in the G-space has an image $d\bar{\mathbf{W}}(\mathbf{u}(\mathbf{x}))$ in the $\bar{G}$-space such that:

$$\begin{aligned} d\mathbf{W}(\mathbf{x}) &= du \cdot \mathbf{x}_u(\mathbf{x}) + dv \cdot \mathbf{x}_v(\mathbf{x}) + dt \cdot \mathbf{x}_t(\mathbf{x}) \\ &\Updownarrow \\ d\bar{\mathbf{W}}(\mathbf{u}(\mathbf{x})) &= du \cdot \mathbf{U} + dv \cdot \mathbf{V} + dt \cdot \mathbf{T} \end{aligned} \tag{27}$$

It is easy to check that the components (du, dv, dt) in Equation (27) are such that

$$\begin{bmatrix} du \\ dv \\ dt \end{bmatrix} = g^{-1}(\mathbf{x}) \cdot \begin{bmatrix} d\mathbf{W}(\mathbf{x}) \cdot \mathbf{x}_u(\mathbf{x}) \\ d\mathbf{W}(\mathbf{x}) \cdot \mathbf{x}_v(\mathbf{x}) \\ d\mathbf{W}(\mathbf{x}) \cdot \mathbf{x}_t(\mathbf{x}) \end{bmatrix} \tag{28}$$

SEDIMENTATION VELOCITY

It is clear that the images of the top and bottom horizons of a layer in the $\bar{G}$-space are parallel horizontal surfaces even though the layer thickness in the G-space is variable. Sedimentation velocity is the key concept introduced in this section to account for these thickness variations, if any.

Sedimentation Velocity $\vartheta(\mathbf{x})$

As shown in Figure 6, let us consider the pages of a book as an analogue of a thin sedimentary layer with a constant thickness Δh bounded by a foot-wall $H_{t-\Delta t}$

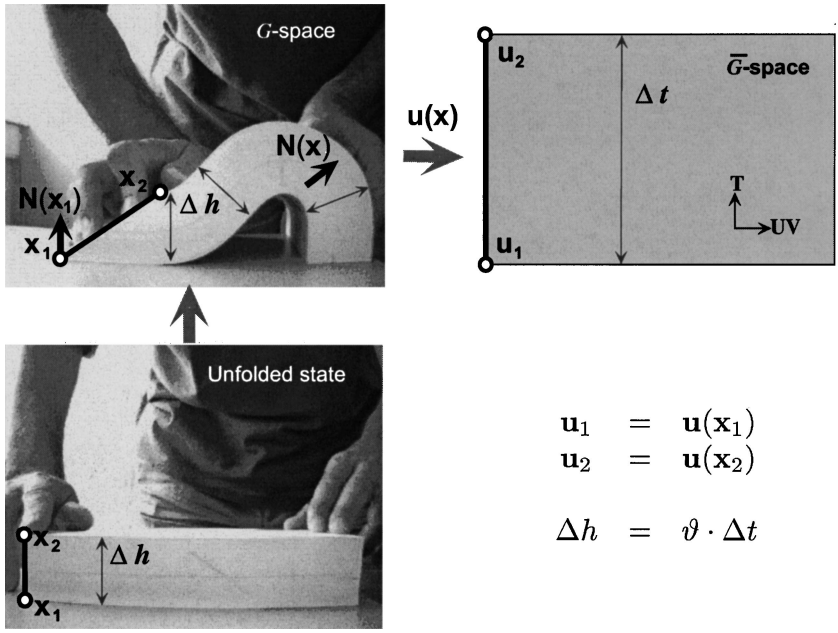

$$\begin{aligned} \mathbf{u}_1 &= \mathbf{u}(\mathbf{x}_1) \\ \mathbf{u}_2 &= \mathbf{u}(\mathbf{x}_2) \\ \Delta h &= \vartheta \cdot \Delta t \end{aligned}$$

Figure 6. Pages of a book viewed as an analog of a geological thin layer folded according to a "flexural slip" style. Note that the thickness Δh in the folded and unfolded states is constant and equal to the sum Δh of the thickness of the pages. Note also that $(\mathbf{x}_1, \mathbf{x}_2)$ is an *IPG*-line whose image in the $\bar{G}$-space is the vertical segment $(\mathbf{u}_1, \mathbf{u}_2)$.

and a hanging-wall H_t. Note that:

- Whether the layer is folded or unfolded, its thickness Δh is the length of a segment orthogonal to H_t and $H_{t-\Delta t}$ and is equal to the sum of the thicknesses of the pages of the book. In other words, provided that there is no compaction and assuming that the layers can slide on each others without generating gaps according to a "flexural slip" tectonic style (e.g., see Couples, Lewis, and Tanner, 1998; Suppe, 1985)) the *thickness* of the layers *is an invariant* throughout geological time whatever the curvilinear coordinate system (u, v, t).
- The gradient of the geological time function $t(\mathbf{x})$ at location $\mathbf{x}$ on H_t is a vector of the G-space such that

$$\mathbf{grad}\, t(\mathbf{x}) \simeq \frac{\Delta t}{\Delta h} \cdot \mathbf{N}(\mathbf{x}) \tag{29}$$

  where $\mathbf{N}(\mathbf{x})$ is the unit normal vector orthogonal to H_t at location $\mathbf{x}$ positively oriented in the direction of the younger terrains (see Eq. 22)).

These observations suggest to introduce the sedimentation velocity $\vartheta(\mathbf{x})$ defined as follows at location $\mathbf{x}$ on H_t:

$$\vartheta(\mathbf{x}) \simeq \frac{\Delta h}{\Delta t} \tag{30}$$

More generally, at the limit when Δt tends towards zero, we deduce from Equations (29) and (30) that the sedimentation velocity $\vartheta(\mathbf{x})$ can be defined as follows at any point $\mathbf{x}$ in the G-space:

$$\vartheta(\mathbf{x}) = \frac{1}{||\mathbf{grad}\, t(\mathbf{x})||} \tag{31}$$

The function $\vartheta(\mathbf{x})$ so defined is an "apparent" sedimentation velocity which represents the "real" sedimentation velocity only if there is no compaction and if the times assigned to the horizons correspond actually to real geological time. Moreover, as shown in Figure 5, from Equations (18), (22), and (31) it can be deduced that, the length of the projection of $\mathbf{x}_t(\mathbf{x})$ onto the direction $\mathbf{N}(\mathbf{x})$ is equal to $\vartheta(\mathbf{x})$:

$$\mathbf{x}_t(\mathbf{x}) \cdot \mathbf{N}(\mathbf{x}) = \vartheta(\mathbf{x}) = \frac{1}{||\mathbf{grad}\, t(\mathbf{x})||} \tag{32}$$

Similarly, it can be deduced from (18) and (31) that:

$$\mathbf{grad}\, t(\mathbf{x}) = \frac{1}{\vartheta(\mathbf{x})} \cdot \mathbf{N}(\mathbf{x}) \tag{33}$$

Decompacted Sedimentation Velocity $\vartheta_\phi(\mathbf{x})$

The sedimentation velocity $\vartheta(\mathbf{x})$ as defined above does not account for the compaction of the terrains which may have occurred from the geological time of deposition to the present time. A column of sediment $\Delta h(\mathbf{x})$ orthogonal to the horizons observed today at location $\mathbf{x}$ in the G-space between two horizons H_t and $H_{t-\Delta t}$ corresponds actually to a vertical column $\Delta H(\mathbf{x})$ at geological time t of deposition such that:

$$\left| \begin{array}{l} \Delta h(\mathbf{x}) = (1 - \phi(\mathbf{x})) \cdot \Delta H(\mathbf{x}) \\ \quad \text{with :} 0 \leq \phi(\mathbf{x}) < 1 \end{array} \right.$$

In this equation, the function $\phi(\mathbf{x})$ is called the "compaction coefficient" and depends both on the trajectory of the particle across geological time and the nature of the sediment observed at location $\mathbf{x}$ (e.g., see Magara, 1976). As a consequence, to account for compaction, the sedimentation velocity $\vartheta(\mathbf{x})$ must be replaced by $\vartheta_\phi(\mathbf{x})$ called the "decompacted sedimentation velocity" and defined as:

$$\vartheta_\phi(\mathbf{x}) = \frac{1}{1 - \phi(\mathbf{x})} \cdot \vartheta(\mathbf{x}) \tag{34}$$

Thickness to Time Conversion

As a direct consequence of definition (30), the thickness of sediments $\Delta h(\mathbf{x})$ observed today at point $\mathbf{x}$ in the G-space and corresponding to a geological time lag Δt, can be deduced as follows from the sedimentation velocity $\vartheta(\mathbf{x})$:

$$\Delta h(\mathbf{x}) = \vartheta(\mathbf{x}) \cdot \Delta t$$

In a similar way, the decompacted thickness $\Delta h_\phi(\mathbf{x})$ of sediments observed today at point $\mathbf{x}$ in the G-space and corresponding to a geological time lag Δt can be deduced as follows from $\vartheta_\phi(\mathbf{x})$:

$$\Delta h_\phi(\mathbf{x}) = \vartheta_\phi(\mathbf{x}) \cdot \Delta t$$

Conversely, the equation above can be used to convert the thickness $\Delta h_\phi(\mathbf{x})$ of a thin layer or a geobody (e.g., a channel or a lens) observed today at location $\mathbf{x}$ in the G-space into a time lag Δt in the $\bar{G}$-space:

$$\Delta t = \frac{\Delta h_\phi(\mathbf{x})}{\vartheta_\phi(\mathbf{x})} \tag{35}$$

ASSESSING DEFORMATIONS IN THE G-SPACE

At geological time t, the horizon H_t was a horizontal plane $\bar{H}_t$ while, for any $\Delta t > 0$, the neighboring horizon $H_{t-\Delta t}$ was then already transformed into a curved surface $\tilde{H}_{t-\Delta t}$ located right below H_t. Moreover, due to gravitation, at geological time t the field of sedimentation velocities was a field of vectors constantly oriented upward relative to the time axis $\mathbf{T}$. As a consequence, to restore the thin layer $\{H_t, H_{t-\Delta t}\}$ located between the horizons H_t and $H_{t-\Delta t}$ as it was at geological time t, one can thus proceed in the $\bar{G}$-space as follows:

- select the horizontal plane $\bar{H}_t$;
- build the curved surface $\tilde{H}_{t-\Delta t}$ deduced from $\bar{H}_t$ as

$$\mathbf{u} = \begin{bmatrix} u \\ v \\ t \end{bmatrix} \in \bar{H}_t \longrightarrow \tilde{\mathbf{u}} = \begin{bmatrix} u \\ v \\ t - \vartheta_\phi \cdot \Delta t \end{bmatrix} \in \tilde{H}_{t-\Delta t} \tag{36}$$

where, for conciseness sake, ϑ_ϕ is set equal to $\vartheta_\phi(\mathbf{x}(\mathbf{u}))$.

The thin layer $\{\bar{H}_t, \tilde{H}_{t-\Delta t}\}$ so defined is the image, at geological time t of deposition, of the thin layer $\{H_t, H_{t-\Delta t}\}$ observed today in the G-space and the transformation R of $\{H_t, H_{t-\Delta t}\}$ into $\{\bar{H}_t, \tilde{H}_{t-\Delta t}\}$ is called a "restoration":

$$\{H_t, H_{t-\Delta t}\} \xrightarrow{R} \{\bar{H}_t, \tilde{H}_{t-\Delta t}\} \tag{37}$$

To characterize this restoration process R for any point $\mathbf{x}$ in the neighborhood of H_t, it is proposed to determine the images $R(\mathbf{x}_u(\mathbf{x}))$, $R(\mathbf{x}_v(\mathbf{x}))$, and $R(\mathbf{x}_t(\mathbf{x}))$ of the vectors $\mathbf{x}_u(\mathbf{x})$, $\mathbf{x}_v(\mathbf{x})$, and $\mathbf{x}_t(\mathbf{x})$, respectively. For this purpose, first observe that according to Equation (11):

$$\mathbf{x}_t(\mathbf{x}) = \lim_{\Delta t \to 0} \frac{\mathbf{x}\big(u(\mathbf{x}), v(\mathbf{x}), t(\mathbf{x})\big) - \mathbf{x}\big(u(\mathbf{x}), v(\mathbf{x}), t(\mathbf{x}) - \Delta t\big)}{\Delta t} \tag{38}$$

Note also that:

$$R\big(\mathbf{x}(u,v,t)\big) = \begin{bmatrix} u \\ v \\ t \end{bmatrix} \quad \text{and} \quad R(\mathbf{x}(u+\Delta u, v+\Delta v, t-\Delta t)) = \begin{bmatrix} u+\Delta u \\ v+\Delta v \\ t-\vartheta_\phi \cdot \Delta t \end{bmatrix}$$

For infinitesimal variations of $\mathbf{x}$, the restoration operator $R(\mathbf{x})$ can always be approximated linearly; according to Equation (38), the image of $\mathbf{x}_t(\mathbf{x})$ in the restored layer $\{\bar{H}_t, \tilde{H}_{t-\Delta t}\}$ is thus a vector $R(\mathbf{x}_t(\mathbf{x}))$ such that:

$$R\big(\mathbf{x}_t(\mathbf{x})\big) = \lim_{\Delta t \to 0} \frac{\begin{bmatrix} u(\mathbf{x}) \\ v(\mathbf{x}) \\ t(\mathbf{x}) \end{bmatrix} - \begin{bmatrix} u(\mathbf{x}) \\ v(\mathbf{x}) \\ t(\mathbf{x}) - \vartheta_\phi \cdot \Delta t \end{bmatrix}}{\Delta t}$$

$$\Downarrow$$

$$R\big(\mathbf{x}_t(\mathbf{x})\big) = \lim_{\Delta t \to 0} \frac{1}{\Delta t} \begin{bmatrix} 0 \\ 0 \\ \vartheta_\phi \cdot \Delta t \end{bmatrix} = \begin{bmatrix} 0 \\ 0 \\ \vartheta_\phi \end{bmatrix} = ||\boldsymbol{\vartheta}_\phi(\mathbf{x})|| \cdot \mathbf{T}$$

Using a similar proof, it can be shown that the images $R(\mathbf{x}_u(\mathbf{x}))$ and $R(\mathbf{x}_v(\mathbf{x}))$ of $\mathbf{x}_u(\mathbf{x})$ and $\mathbf{x}_v(\mathbf{x})$ in the restored layer $\{\bar{H}_t, \tilde{H}_{t-\Delta t}\}$ are constant vectors equal to $\mathbf{U}$ and $\mathbf{V}$, respectively. To sum up, for any point $\mathbf{x}$ in the G-space:

- the image of $\mathbf{x}_u(\mathbf{x})$ at geological time of deposition is the vector $\mathbf{U}$;
- the image of $\mathbf{x}_v(\mathbf{x})$ at geological time of deposition is the vector $\mathbf{V}$;
- the image of $\mathbf{x}_t(\mathbf{x})$ at geological time of deposition is the vector $\tilde{\mathbf{T}}(\mathbf{x}) = \boldsymbol{\vartheta}_\phi(\mathbf{x}) \cdot \mathbf{T}$.

The metric properties of the folded state observed today in the neighborhood of $\mathbf{x}$ are characterized by the metric tensor $g(\mathbf{x})$ associated with the local G-frame $(\mathbf{x}_u(\mathbf{x}), \mathbf{x}_v(\mathbf{x}), \mathbf{x}_t(\mathbf{x}))$ and defined by the Equation (19). Similarly, the vectors $(\mathbf{U}, \mathbf{V}, \tilde{\mathbf{T}}(\mathbf{x}))$ constitute a local frame associated with the following metric tensor $g_0(\mathbf{x})$ characterizing the metric properties of the neighborhood of the image of $\mathbf{x}$ in the restored state at geological time of deposition:

$$\begin{aligned} g_0(\mathbf{x}) &= \begin{bmatrix} ||\mathbf{U}||^2 & \mathbf{U}\cdot\mathbf{V} & \mathbf{U}\cdot\tilde{\mathbf{T}}(\mathbf{x}) \\ \mathbf{V}\cdot\mathbf{U} & ||\mathbf{V}||^2 & \mathbf{V}\cdot\tilde{\mathbf{T}}(\mathbf{x}) \\ \tilde{\mathbf{T}}(\mathbf{x})\cdot\mathbf{U} & \tilde{\mathbf{T}}(\mathbf{x})\cdot\mathbf{V} & ||\tilde{\mathbf{T}}(\mathbf{x})||^2 \end{bmatrix} \\ &= \begin{bmatrix} 1 & 0 & 0 \\ 0 & 1 & 0 \\ 0 & 0 & |\boldsymbol{\vartheta}_\phi(\mathbf{x})|^2 \end{bmatrix} \end{aligned} \tag{39}$$

The 3D strain tensor $\mathcal{E}(\mathbf{x})$ characterizing the deformations of the G-space in the neighborhood of $\mathbf{x}$ between geological time of deposition and present time is then defined as follows (e.g., see Mallet, 2002; Sedov, 1975; Sokolnikoff, 1964):

$$\mathcal{E}(\mathbf{x}) = \begin{bmatrix} \mathcal{E}_{uu} & \mathcal{E}_{uv} & \mathcal{E}_{u\tilde{t}} \\ \mathcal{E}_{vu} & \mathcal{E}_{vv} & \mathcal{E}_{v\tilde{t}} \\ \mathcal{E}_{\tilde{t}u} & \mathcal{E}_{\tilde{t}v} & \mathcal{E}_{\tilde{t}\tilde{t}} \end{bmatrix} = \frac{1}{2} \cdot (g(\mathbf{x}) - g_0(\mathbf{x})) \tag{40}$$

Observe that the components of $\mathcal{E}(\mathbf{x})$ depend strongly on the 3D curvilinear coordinate system induced by the functions $u(\mathbf{x})$, $v(\mathbf{x})$, and $t(\mathbf{x})$. However, it can be shown (e.g., see Mallet, 2002; Sokolnikoff, 1964) that there are entities linked to $g(\mathbf{x})$ and $g_0(\mathbf{x})$ which are invariant if the scale of geological time t is changed or if the paleogeographic coordinates (u, v) are rotated and translated according to Equation (7). For example, consider an infinitely small element of volume dV at location $\mathbf{x}$ in the infinitely thin layer $\{H_t, H_{t-\Delta t}\}$ and its image dV_0 at deposition time t in the layer $\{\bar{H}_t, \tilde{H}_{t-\Delta t}\}$: it can be shown (e.g., see Mallet, 2002, p. 395) that the cubic dilatation coefficient θ defined by

$$\theta(\mathbf{x}) = \frac{dV - dV_0}{dV_0} \tag{41}$$

is an invariant which can be computed as follows:

$$\theta(\mathbf{x}) = \sqrt{\frac{\det(g(\mathbf{x}))}{\det(g_0(\mathbf{x}))}} - 1 = \sqrt{\frac{\det(g_0^{-1}(\mathbf{x}))}{\det(g^{-1}(\mathbf{x}))}} - 1 \tag{42}$$

Taking into account Equations (21), (39), (34), and (22), it can be concluded that:

$$\theta(\mathbf{x}) = \frac{1 - \phi(\mathbf{x})}{|(\mathbf{grad}\, u(\mathbf{x}) \times \mathbf{grad}\, v(\mathbf{x})) \cdot \mathbf{N}(\mathbf{x})|} - 1 \tag{43}$$

The above formulae clearly shows that $\theta(\mathbf{x})$ is actually invariant if the scale of geological time t is changed or if the paleogeographic coordinates (u, v) are rotated and translated. There are also other invariants characterizing the "Principal Strain Directions" at any location $\mathbf{x}$ in the G-space which are deduced from the eigen vectors $\{D_{(1)}(\mathbf{x}), D_{(2)}(\mathbf{x}), D_{(3)}(\mathbf{x})\}$ and eigen values $\{\lambda_{(1)}(\mathbf{x}), \lambda_{(2)}(\mathbf{x}), \lambda_{(3)}(\mathbf{x})\}$ of matrix $S(\mathbf{x}) = g^{-1}(\mathbf{x}) \cdot \mathcal{E}(\mathbf{x})$ called the "Eulerian strain tensor":

$$\underbrace{(g^{-1}(\mathbf{x}) \cdot \mathcal{E}(\mathbf{x}))}_{S(\mathbf{x})} \cdot D_{(i)}(\mathbf{x}) = \lambda_{(i)}(\mathbf{x}) \cdot D_{(i)}(\mathbf{x}) \quad \forall\, i = 1, 2, 3 \tag{44}$$

For example, consider an infinitely small segment $d\mathbf{x} = \mathbf{W} \cdot ||d\mathbf{x}||$ at location $\mathbf{x}$ in the infinitely thin layer $\{H_t, H_{t-\Delta t}\}$ and its image $d\mathbf{x}_0$ at deposition time in the layer $\{\bar{H}_t, \tilde{H}_{t-\Delta t}\}$. Assuming that $\mathbf{W}$ is a unit vector, the elongation coefficient $e(\mathbf{W})$ defined as follows is clearly a function of the orientation of this vector:

$$e(\mathbf{W}) = \frac{||d\mathbf{x}|| - ||d\mathbf{x}_0||}{||d\mathbf{x}_0||} \tag{45}$$

It can be shown (e.g., see Mallet, 2002, p. 396) that $e(\mathbf{W})$ is extremum when $\mathbf{W}$ is equal to one of the three directions $\{\mathbf{W}_{(i)}(\mathbf{x})\}$ defined as follows where $(D^u_{(i)}(\mathbf{x}), D^v_{(i)}(\mathbf{x}), D^t_{(i)}(\mathbf{x}))$ are the three components of the eigen vector $D_{(i)}(\mathbf{x})$ of $S(\mathbf{x})$:

$$\mathbf{W}_{(i)} = \frac{D^u_{(i)} \cdot \mathbf{x}_u + D^v_{(i)} \cdot \mathbf{x}_v + D^t_{(i)} \cdot \mathbf{x}_t}{||D^u_{(i)} \cdot \mathbf{x}_u + D^v_{(i)} \cdot \mathbf{x}_v + D^t_{(i)} \cdot \mathbf{x}_t||} \quad \forall i = 1, 2, 3 \tag{46}$$

These vectors $\{\mathbf{W}_{(i)}(\mathbf{x})\}$ of the G-space are called "Principal Strain Directions" and it can be shown (Mallet, 2002) that they are orthogonal and independent from the parametrization $(u(\mathbf{x}), v(\mathbf{x}), t(\mathbf{x}))$. The elongations $\{e_{(i)}(\mathbf{x}) = e(\mathbf{W}_{(i)})\}$ corresponding to the principal strain directions are also invariants and are deduced from the eigen values of $S(\mathbf{x})$ as follows:

$$e_{(i)}(\mathbf{x}) = \frac{1}{\sqrt{1 - 2 \cdot \lambda_{(i)}(\mathbf{x})}} - 1 \quad \forall i = 1, 2, 3 \tag{47}$$

In practice, all these invariants can be considered as "structural attributes" which may be linked to the fracturation of the terrains and the variations of the physical properties to be interpolated. For example, the permeability of the terrains is positively correlated to the fracturation if there is no cementation posterior to the generation of the fractures, otherwise it may be negatively correlated. As a consequence, to account for postdepositional variations of the properties induced by the fracturation, one could, for example, use co-Kriging based on the above invariants rather than an ordinary or simple Kriging method (e.g., see Chiles and Delfiner, 1999; Deutsch and Journel, 1998; Goovaerts, 1997; Mallet, 2002).

Comment

Classically, balanced restoration methods used in structural geology proceed in two steps (e.g., see Dahlstrom, 1969; Gibbs, 1983; Mallet, 2002; Suppe 1985):

1. first, the top horizon is unfolded;

2. next, the stack of layers (below the top horizon) is unfolded to follow the movement of the top horizon while preserving the mass of the terrains.

It should be observed that the GeoChron method proposed above to compute the strain tensor and its associated invariants must not be mistaken with restoration methods for the following reasons:

- Contrary to classical restoration methods, in the GeoChron method the layers in the *G*-space are not actually unfolded.
- Contrary to classical restoration methods, in the GeoChron method the strain tensor and its associated invariants represent the *total* deformation at any depth in the subsurface. Classical restoration methods only unfold the neighborhood of the top horizon completely which implies that, with these methods, the strain tensor can be evaluated correctly only in the neighborhood of this top horizon: residual deformation in deeper regions of the subsurface are not taken into account by these methods directly.

Several types of balanced restoration have been described in the literature like, for example, the flexural slip and incline shear methods (Gibbs, 1983; Suppe, 1985). It should be observed that, in the GeoChron model, the choice of the field of *IPG*-lines is a "model decision" which is equivalent to the choice of a particular type of restoration.

INTRINSIC CONSTRAINTS FOR u(x)

The primary purpose of this article is to introduce a mathematical framework designed for modeling properties in sedimentary geology, not to provide a technique to actually build such a framework. Even though building $\mathbf{u}(\mathbf{x})$ in practical applications is beyond the scope of this article, it is possible to explicit some general "intrinsic" constraints to be honored by the components $u(\mathbf{x})$, $v(\mathbf{x})$, and $t(\mathbf{x})$ of $\mathbf{u}(\mathbf{x})$ whatever the shape of the geological structures in the *G*-space. In this section we present a series of such intrinsic constraints which must be used to restrain the set of possible functions $u(\mathbf{x})$, $v(\mathbf{x})$, and $t(\mathbf{x})$ and thus help in designing methods to actually build $\mathbf{u}(\mathbf{x})$ in practical applications.

Intrinsic Piecewise Continuity Constraint

The GeoChron model presented in this article implicitly assumes that the components $u(\mathbf{x})$, $v(\mathbf{x})$, and $t(\mathbf{x})$ of $\mathbf{u}(\mathbf{x})$ are piecewise continuous (and derivable) functions in the *G*-space. The only discontinuity which can affect these functions correspond to fault surfaces and unconformity surfaces. As a consequence, this

induces a piecewise continuity constraint which must be honored by any interpolation method used to compute a valid transformation $\mathbf{u}(\mathbf{x})$.

Intrinsic *IPG* Constraints

It can be observed that any *IPG*-line is the intersection of an isovalue surface of the function $u(\mathbf{x})$ with an isovalue surface of the function $v(\mathbf{x})$. As a consequence, for any given *IPG*-line L, the functions $u(\mathbf{x})$ and $v(\mathbf{x})$ should honor the following intrinsic constraints called the "*IPG*" constraints:

$$\forall \mathbf{x} \in L : \left| \begin{array}{l} u(\mathbf{x}) = u^L \\ v(\mathbf{x}) = v^L \\ t(\mathbf{x}) = t(\mathbf{x}|L) \end{array} \right. \tag{48}$$

In this constraints:

- (u^L, v^L) is a pair of constants depending only on L (see Fig. 7).
- $t(\mathbf{x}|L)$ is a function interpolating the values of the geological time observed at the intersections of L with the horizons $\{H_{t_0}, H_{t_1}, \cdots, H_{t_n}\}$.

Intrinsic Iso-Geological-Time Constraints

By definition, a horizon H_t corresponds to a set of particles deposited at the same geological time t. As a consequence, for any horizon H_{t_i}, the function $t(\mathbf{x})$

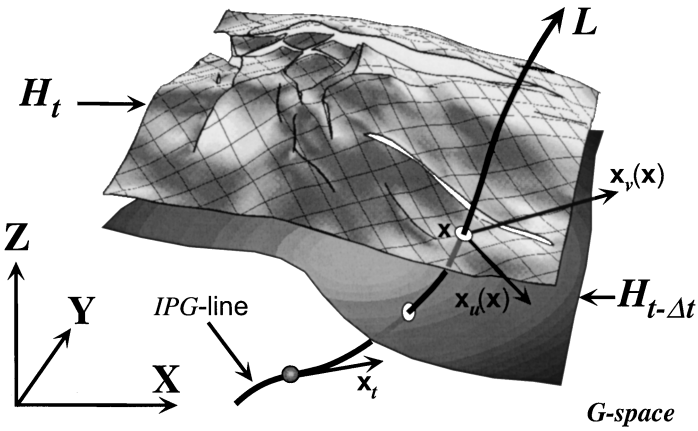

Figure 7. Intrinsic constraints are controlled by the geometry of the horizons and *IPG*-lines in the G-space. Note that u-lines and v-lines are contained in H_t and are tangent to $\mathbf{x}_u$ and $\mathbf{x}_v$, respectively, while $\mathbf{x}_t$ is tangent to an *IPG*-line.

should honor the following intrinsic constraints called the "iso-geological-time" constraints (see Fig. 7):

$$\forall \mathbf{x} \in H_{t_i} : t(\mathbf{x}) = t_i \tag{49}$$

Intrinsic Flexural Slip Constraint

Restricting the two first components $(u(\mathbf{x}), v(\mathbf{x}))$ of the $\bar{G}$-parametrization $\mathbf{u}(\mathbf{x})$ to points $\mathbf{x}$ located on a horizon H_τ amounts to a parametrization of this horizon, called the "induced parametrization" of H_τ. The properties of this induced parametrization are linked to the properties of $\mathbf{u}(\mathbf{x})$ and can thus be used to constrain $\mathbf{u}(\mathbf{x})$ in a way consistent with the geological processes which generated H_τ throughout geological time.

First, observe that the image of H_τ in the 2D parametric domain of the induced parametrization is the horizontal plane $\bar{H}_\tau$ which can be seen as an unfolded/unfaulted version of H_τ. As a consequence, for any point $\mathbf{x}$ on H_τ, the vectors $\mathbf{x}_u(\mathbf{x})$ and $\mathbf{x}_v(\mathbf{x})$ are tangent to H_τ and the 2D metric tensor $g(\mathbf{x}|H_\tau)$ of H_τ associated with the induced parametrization at location $\mathbf{x}$ on H_τ is such that (DoCarmo, 1976; Mallet, 2002):

$$g(\mathbf{x}|H_\tau) = \begin{bmatrix} ||\mathbf{x}_u(\mathbf{x})||^2 & \mathbf{x}_u(\mathbf{x}) \cdot \mathbf{x}_v(\mathbf{x}) \\ \mathbf{x}_v(\mathbf{x}) \cdot \mathbf{x}_u(\mathbf{x}) & ||\mathbf{x}_v(\mathbf{x})||^2 \end{bmatrix} \tag{50}$$

Similarly, the metric tensor $g_0(\mathbf{x}|H_\tau)$ of $\bar{H}_\tau$ associated with the induced parametrization at location $\mathbf{u}(\mathbf{x})$ is such that:

$$g_0(\mathbf{x}|H_\tau) = \begin{bmatrix} ||\mathbf{U}||^2 & \mathbf{U} \cdot \mathbf{V} \\ \mathbf{V} \cdot \mathbf{U} & ||\mathbf{V}||^2 \end{bmatrix} = \begin{bmatrix} 1 & 0 \\ 0 & 1 \end{bmatrix} \tag{51}$$

The 2D deformation of the surface H_τ between geological time of deposition τ and present time is then characterized by the 2D strain tensor $\mathcal{E}(\mathbf{x}|H_\tau)$ defined as (e.g., see Mallet 2002; Sedov, 1975; Sokolnikoff, 1964):

$$\mathcal{E}(\mathbf{x}|H_\tau) = \begin{bmatrix} \mathcal{E}_{uu} & \mathcal{E}_{uv} \\ \mathcal{E}_{vu} & \mathcal{E}_{vv} \end{bmatrix} = \frac{1}{2} \cdot (g(\mathbf{x}|H_\tau) - g_0(\mathbf{x}|H_\tau)) \tag{52}$$

Let us assume now that the studied geological layers have been folded according to a "flexural slip" tectonic style (e.g., see Couples, Lewis, and Tanner, 1998; Suppe, 1985; and Fig. 6) without any compaction. In such a case:

- the 2D deformation of H_τ should be minimum;
- the variation of volume in the neighborhood of H_τ should be minimum.

In other words, the magnitude of the components of $\mathcal{E}(\mathbf{x}|H_\tau)$ defined by Equation (52) and the magnitude of the compaction $\phi(x)$ and the cubic dilatation $\theta(\mathbf{x})$ defined by Equation (43) should be as small as possible for any point $\mathbf{x}$ on H_τ. As a consequence, we conclude that $u(\mathbf{x})$ and $v(\mathbf{x})$ should honor the following intrinsic constraints that we propose to call the "flexural slip" constraints:

$$\forall \mathbf{x} \in H_\tau : \left| \begin{array}{ll} 1) & ||\mathbf{x}_u(\mathbf{x})||^2 \simeq ||\mathbf{x}_v(\mathbf{x})||^2 \simeq 1 \\ 2) & \mathbf{x}_u(\mathbf{x}) \cdot \mathbf{x}_v(\mathbf{x}) \simeq 0 \\ 3) & \theta(\mathbf{x}) = 0 \text{ and } \phi(\mathbf{x}) = 0 \end{array} \right. \tag{53}$$

Let us introduce the projections $\mathbf{grad}_H u(\mathbf{x})$ and $\mathbf{grad}_H v(\mathbf{x})$ of the gradients $\mathbf{grad}\, u(\mathbf{x})$ and $\mathbf{grad}\, v(\mathbf{x})$ onto the horizon $H \equiv H_\tau$:

$$\forall \mathbf{x} \in H_\tau : \left| \begin{array}{l} \mathbf{grad}_H u(\mathbf{x}) = \mathbf{grad}\, u(\mathbf{x}) - \{\mathbf{grad}\, u(\mathbf{x}) \cdot \mathbf{N}(\mathbf{x})\} \cdot \mathbf{N}(\mathbf{x}) \\ \mathbf{grad}_H v(\mathbf{x}) = \mathbf{grad}\, v(\mathbf{x}) - \{\mathbf{grad}\, v(\mathbf{x}) \cdot \mathbf{N}(\mathbf{x})\} \cdot \mathbf{N}(\mathbf{x}) \end{array} \right. \tag{54}$$

It can be observed that:

$$\begin{aligned} \mathbf{grad}_H u(\mathbf{x}) \cdot \mathbf{grad}_H v(\mathbf{x}) = \mathbf{grad}\, u(\mathbf{x}) \cdot \mathbf{grad}\, v(\mathbf{x}) \\ - \{\mathbf{grad}\, u(\mathbf{x}) \cdot \mathbf{N}(\mathbf{x})\} \cdot \{\mathbf{grad}\, v(\mathbf{x}) \cdot \mathbf{N}(\mathbf{x})\} \end{aligned} \tag{55}$$

Moreover, using the formula

$$(\mathbf{a} \times \mathbf{b}) \cdot (\mathbf{c} \times \mathbf{d}) = (\mathbf{a} \cdot \mathbf{c}) \cdot (\mathbf{b} \cdot \mathbf{d}) - (\mathbf{b} \cdot \mathbf{c}) \cdot (\mathbf{a} \cdot \mathbf{d})$$

and the definitions (18) and (22), it can also be checked that:

$$\left| \begin{array}{ll} ||\mathbf{x}_u(\mathbf{x})||^2 & = \dfrac{1}{D(\mathbf{x})} \cdot \{||\mathbf{grad}\, v(\mathbf{x})||^2 - |\mathbf{grad}\, v(\mathbf{x}) \cdot \mathbf{N}(\mathbf{x})|^2\} \\ ||\mathbf{x}_v(\mathbf{x})||^2 & = \dfrac{1}{D(\mathbf{x})} \cdot \{||\mathbf{grad}\, u(\mathbf{x})||^2 - |\mathbf{grad}\, u(\mathbf{x}) \cdot \mathbf{N}(\mathbf{x})|^2\} \\ \mathbf{x}_u(\mathbf{x}) \cdot \mathbf{x}_v(\mathbf{x}) & = -\dfrac{1}{D(\mathbf{x})} \cdot \{\mathbf{grad}\, u(\mathbf{x}) \cdot \mathbf{grad}\, v(\mathbf{x}) - \{\mathbf{grad}\, u(\mathbf{x}) \cdot \mathbf{N}(\mathbf{x})\} \cdot \{\mathbf{grad}\, v(\mathbf{x}) \cdot \mathbf{N}(\mathbf{x})\}\} \end{array} \right. \tag{56}$$

with:

$$D(\mathbf{x}) = |\{\mathbf{grad}\, u(\mathbf{x}) \times \mathbf{grad}\, v(\mathbf{x})\} \cdot \mathbf{N}(\mathbf{x})|^2 \tag{57}$$

Note that, according to equation (43):

$$\{\theta(\mathbf{x}) = \phi(\mathbf{x}) = 0\} \Rightarrow D(\mathbf{x}) = 1$$

From Equations (55) and (56), we can thus write:

$$\begin{aligned} ||\mathbf{x}_u(\mathbf{x})||^2 &= \frac{1}{D(\mathbf{x})} \cdot ||\mathbf{grad}_H v(\mathbf{x})||^2 \\ ||\mathbf{x}_v(\mathbf{x})||^2 &= \frac{1}{D(\mathbf{x})} \cdot ||\mathbf{grad}_H u(\mathbf{x})||^2 \\ \mathbf{x}_u(\mathbf{x}) \cdot \mathbf{x}_v(\mathbf{x}) &= -\frac{1}{D(\mathbf{x})} \cdot \mathbf{grad}_H u(\mathbf{x}) \cdot \mathbf{grad}_H v(\mathbf{x}) \end{aligned} \tag{58}$$

From Equations (57) and (58), at any point $\mathbf{x}$ in the G-space where there is no variation of volume ($\theta(\mathbf{x}) = \phi(\mathbf{x}) = 0$), it can be concluded that the intrinsic flexural slip constraints defined by Equations (53) are equivalent to the following constraints where $H \equiv H(\mathbf{x})$ represents the horizon passing by the point $\mathbf{x}$:

$$\forall\, \mathbf{x} \in G : \begin{vmatrix} 1)\ ||\mathbf{grad}_H u(\mathbf{x})|| \simeq ||\mathbf{grad}_H v(\mathbf{x})|| \simeq 1 \\ 2) \qquad \mathbf{grad}_H u(\mathbf{x}) \cdot \mathbf{grad}_H v(\mathbf{x}) \simeq 0 \end{vmatrix} \tag{59}$$

It is important to note that, specifying a flexural slip tectonic style, thanks to these constraints, implicitly specifies the shape of the *IPG*-lines. As a consequence, the flexural slip constraints and the *IPG*-lines constraints presented above should not be used simultaneously.

APPLICATION TO PROPERTY MODELING

As mentioned in the introduction, the primary purpose of this article is to propose a mathematical framework for building a consistent coordinate system for modeling properties in the subsurface. In the following we show how the GeoChron model introduced in the previous sections can be used to model properties at different scales of resolution.

Property Modeling in the $\bar{G}$-Space

Consider a particle of sediment observed today at location $\mathbf{x}$ on the horizon H_t and let $\varphi(\mathbf{x})$ be a physical property attached to this particle. According to Equation (6), if it can be assumed that this property was kept unchanged throughout geological time (no diagenesis), then there exists a function $\bar{\varphi}(\mathbf{u})$ defined in the $\bar{G}$-space such that:

$$\varphi(\mathbf{x}) \equiv \bar{\varphi}(\mathbf{u}(\mathbf{x})) \tag{60}$$

At geological time t of deposition of H_t, the spatial variation of $\overline{\varphi}(\mathbf{u})$ on $\overline{H}_t$ depends strongly on the paleoenvironment $e_t(u, v)$ which is also a function of the $\overline{G}$-coordinates. Even though postdepositional transformations (such as diagenesis) do occur, the present day variation of $\varphi(\mathbf{x})$ still depends strongly on the paleoenvironment $e_t(u, v)$. Moreover, if the components $u(\mathbf{x})$ and $v(\mathbf{x})$ of $\mathbf{u}(\mathbf{x})$ honor the intrinsic minimum deformation constraints (see Eq. (53)), then the geodesic curvilinear distances, the angles and areas on any horizon H_t, are all approximately equal to their Euclidean images on the plane $\overline{H}_t$ in the $\overline{G}$-space. Consequently, the modeling of a property by any method, including Discrete Smooth Interpolation (DSI) (Mallet, 2002) and geostatistics (Chiles and Delfiner, 1999; Deutsch and Journel, 1998; Goovaerts, 1997; Journal and Huijbregt, 1978; Mallet, 2002; Matheron, 1968), is better performed in the $\overline{G}$-space instead of the G-space.

In practice, to model the variations of $\varphi(\mathbf{x})$ in the G-space in a way consistent with the sedimentation process, it is thus proposed to proceed as follows:

1. Collect a set of pairs $\{\mathbf{x}_k, \varphi(\mathbf{x}_k) : k = 1, 2, \cdots, K\}$ corresponding to *present day* values of $\varphi(\mathbf{x})$ observed on a set of sampling points $\{\mathbf{x}_k\}$ in the G-space.
2. For any data point $\{\mathbf{x}_k, \varphi(\mathbf{x}_k)\}$ observed in the G-space, build its image $\{\mathbf{u}_k = \mathbf{u}(\mathbf{x}_k), \overline{\varphi}(\mathbf{u}_k) = \varphi(\mathbf{x}_k)\}$ in the $\overline{G}$-space. Note that, if the present day values $\varphi(\mathbf{x}_k)$ are affected by diagenesis, then these postdepositional modifications will be implicitly taken into account by any interpolation of the values $\overline{\varphi}(\mathbf{u}_k)$ in the G-space.
3. In the $\overline{G}$-space (see Fig. 2), build a rectilinear regular 3D grid $\overline{\mathcal{G}}$ such that:
   (a) $\overline{\mathcal{G}}$ covers, in the $\overline{G}$-space, the image of the domain of interest which was originally chosen in the G-space,
   (b) the axes of $\overline{\mathcal{G}}$ are aligned with the ($\mathbf{U}$, $\mathbf{V}$, $\mathbf{T}$) vectors defining the orientation of the geostationary camera,
   (c) the grid $\overline{\mathcal{G}}$ is assumed to be fine enough to capture the scale of resolution of the variations of $\overline{\varphi}(\mathbf{u})$.

4. Using a geostatistical method or the DSI method (Mallet, 2002), build an estimation of $\overline{\varphi}(\mathbf{u})$ at all nodes of $\overline{\mathcal{G}}$. If needed, these interpolation methods (e.g., collocated co-Kriging) can be tuned to account for postdepositional transformations of this property induced, for example, by diagenesis or fractures correlated to the invariants of the strain tensor.
5. At any point $\mathbf{x}$ where the value of $\varphi(\mathbf{x})$ is needed, proceed as follows:
   (a) determine the cell $\overline{C}(\mathbf{u})$ of $\overline{\mathcal{G}}$ where the image $\mathbf{u} = \mathbf{u}(\mathbf{x})$ is located,
   (b) use a local interpolator (e.g., see Mallet, 2002; Mortenson, 1985) to determine the value of $\overline{\varphi}(\mathbf{u})$ from the values previously estimated at the vertices of $\overline{C}(\mathbf{u})$,
   (c) return the value $\varphi(\mathbf{x}) = \overline{\varphi}(\mathbf{u}(\mathbf{x}))$.

Note that this procedure, never uses the function $\mathbf{x}(\mathbf{u})$ transforming a point $\mathbf{u}$ of the $\overline{G}$-space into a point $\mathbf{x}$ of the G-space. Thus, it works even if there exists some eroded parts in the studied domain (see Fig. 4). Moreover, from a practical point of view, it can be observed that:

1. as opposed to $\varphi(\mathbf{x})$, the function $\overline{\varphi}(\mathbf{u})$ is not affected by discontinuities induced by faults and unconformities, if any;
2. as opposed to $\varphi(\mathbf{x})$, the function $\overline{\varphi}(\mathbf{u})$ is not affected by the folding of the horizons, if any;
3. as opposed to $\varphi(\mathbf{x})$, the function $\overline{\varphi}(\mathbf{u})$ is not affected by eroded zones, if any;
4. in the $\overline{G}$-space, to simplify the implementation of geostatistical methods, it is always possible to rotate the (u, v) coordinate system to align it with the principal directions of anisotropy of $\overline{\varphi}(\mathbf{u})$, if any.

Why Using the GeoChron Model ?

It is now possible to point out some important benefits that one can expect from using the GeoChron model to interpolate properties in the subsurface:

1. From a theoretical point of view, modeling the properties in the $\overline{G}$-space rather than in the G-space short cuts the complexity induced by the geometry of the geological structures: in a sense, using the GeoChron model, we have simplified the "geological equation." This is quite similar to the common practice used to get rid of a known solution when solving an algebraic equation: if a trivial solution x^* is known (equivalent to the geometry of our geological structures), then a simpler equation having the same remaining solutions can be obtained by dividing the original equation by $(x - x^*)$.
2. From a computer-science point of view, the storage of the property in the rectilinear regular 3D grid $\overline{\mathcal{G}}$ covering the $\overline{G}$-space is very efficient for the three following reasons:
   - Many modern geostatistical software (Deutsch and Journal, 1998) make an intensive use of rectilinear regular grids. As a consequence, these geostatistical tools can be used without any modification to interpolate a property $\overline{\varphi}(\mathbf{u})$ on the grid $\overline{\mathcal{G}}$ in the $\overline{G}$-space.
   - Contrary to curvilinear grids (see Figs. 1 and 8), there is no need for storing the coordinates and the connectivities of the nodes of $\overline{\mathcal{G}}$. This allows a very simple and compact storage of $\overline{\varphi}(\mathbf{u})$ in a 3D array whose entries correspond to the nodes of $\overline{\mathcal{G}}$.
   - Compact storage of $\overline{\varphi}(\mathbf{u})$ in the grid $\overline{\mathcal{G}}$ allows the steps of this rectilinear regular grid to be chosen very small to model fine variations of $\overline{\varphi}(\mathbf{u})$.

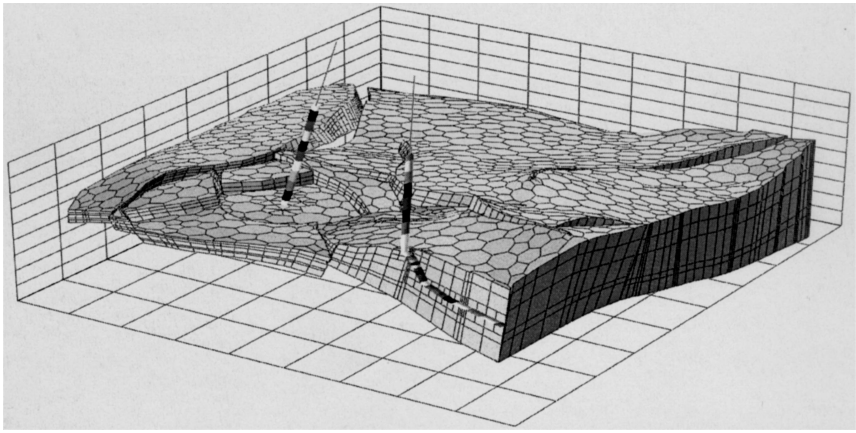

Figure 8. Example of decomposition of a reservoir into a set of polyhedric adjacent 3D cells adapted to the specific needs of a flow simulator. Note that the edges of the cells never cross the horizons and the faults surfaces.

3. From a practical point of view, it can be observed that property modeling based on the GeoChron model is independent from any grid covering the G-space. As a consequence, it is possible to build a *unified* property model whatever its future uses to populate different types of grids. For any specific type of grid required in the G-space by a particular application, it is thus possible to:
   - build the application grid *after* the modeling of the properties;
   - adapt, locally, the geometry of the application grid to the variations of the properties.

Upscaling

In reservoir engineering, oil and gas reservoirs located in the G-space are often decomposed into a set of adjacent polyhedric 3D cells, called "flow-cells," whose edges never cross the faults or the horizons (see Figs. 1 and 8). In practice, the geometry of these cells is adapted to the specific needs of the flow simulator and a common problem consists in populating each cell with a field of permeabilities corresponding to the terrains it contains. Note that the average size of these flow-cells is typically an order of magnitude larger than the frequency of the variations of these permeabilities. As a consequence, for each flow-cell, a process called "upscaling" must be used to replace the set of all within-cell permeabilities by a unique cell-permeability tensor. Many techniques have been proposed in the literature (e.g., see Chiles and Delfiner, 1999; Darman and others, 2000; Gautier, Blunt, and Christie 1999; Renard and de Marsily, 1997, Wen and others, 2003;

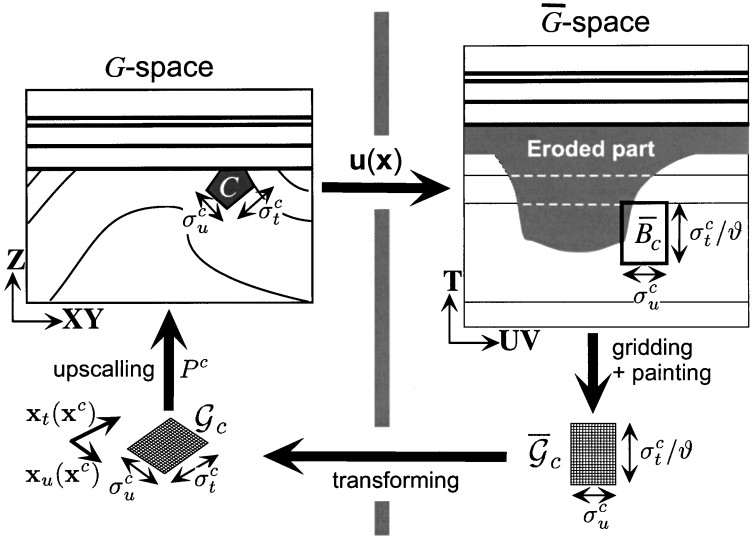

Figure 9. Upscaling the permeabilities of a cell C in the $\overline{G}$-space: The cell C centered on $\mathbf{x}^c$ in the G-space is associated with a box $\overline{B}_c$ which is centered on $\mathbf{u}(\mathbf{x}^c)$ and whose edges are parallel to the $(\mathbf{U}, \mathbf{V}, \mathbf{T})$ directions in the $\overline{G}$-space. Note that $\overline{B}_c$ may overlap eroded or faulted regions without introducing artifacts in the upscaling process.

Trykozko, Zijl, and Bossavit, 2001) and all of them assume that the variations of scalar permeabilities are known in each flow-cell.

Modeling the field of scalar permeabilities directly in the $\overline{G}$-space allows these upscaling methods to be implemented in a very simple way for any polyhedric flow-cell C defined in the G-space. For this purpose, assuming C small enough to ensure that $\mathbf{x}_u(\mathbf{x})$, $\mathbf{x}_v(\mathbf{x})$, and $\mathbf{x}_t(\mathbf{x})$ are approximately constant within C, we suggest to proceed as follows (see Fig. 9):

1. Look for the center of gravity $\mathbf{x}^c$ of C and determine its image $\mathbf{u}^c = \mathbf{u}(\mathbf{x}^c)$ in the $\overline{G}$-space.
2. Determine the sizes σ_u^c, σ_v^c, and σ_t^c of C in the directions parallel to $\mathbf{x}_u(\mathbf{x}^c)$, $\mathbf{x}_v(\mathbf{x}^c)$, and $\mathbf{x}_t(\mathbf{x}^c)$, respectively.
3. In the $\overline{G}$-space, build an hexahedral box $\overline{B}_c$ centered on $\mathbf{u}^c$ whose edges are parallel to the $(\mathbf{U}, \mathbf{V}, \mathbf{T})$ vectors and have sizes such that:
   - $\Delta_u^c = \sigma_u^c$ is the size of $\overline{B}_c$ in the direction $\mathbf{U}$;
   - $\Delta_v^c = \sigma_u^c$ is the size of $\overline{B}_c$ in the direction $\mathbf{V}$;
   - $\Delta_t^c = \sigma_t^c / ||\vartheta_\phi(\mathbf{x}^c)||$ is the size of $\overline{B}_c$ in the direction $\mathbf{T}$ (see Eq. (35)).
4. Cover $\overline{B}_c$ with a rectilinear regular 3D grid $\overline{\mathcal{G}}_c$ corresponding to the part of the fine 3D grid $\overline{\mathcal{G}}$ covering the $\overline{G}$-space and contained in the box $\overline{B}_c$ (see Figs. 2B and 9).

5. "Paint" the hexahedral "microcells" of $\bar{\mathcal{G}}_c$ with the permeabilities $\bar{\varphi}(\mathbf{u})$ previously computed and stored in $\bar{\mathcal{G}}$.
6. Transform the rectilinear regular 3D grid $\bar{\mathcal{G}}_c$ into a rectilinear regular 3D grid $\mathcal{G}_c$ located in the G-space and such that:
   - the edges of $\mathcal{G}_c$ are parallel to $\mathbf{x}_u(\mathbf{x}^c)$, $\mathbf{x}_v(\mathbf{x}^c)$, and $\mathbf{x}_t(\mathbf{x}^c)$, respectively (note that, although the edges of $\bar{\mathcal{G}}_c$ are orthogonal, this is generally not the case for the edges of $\mathcal{G}_c$);
   - the sizes of $\mathcal{G}_c$ in the $\mathbf{x}_u(\mathbf{x}^c)$, $\mathbf{x}_v(\mathbf{x}^c)$, and $\mathbf{x}_t(\mathbf{x}^c)$ directions are equal to σ_u^c, σ_v^c, and σ_t^c, respectively;
   - the numbers of nodes of $\mathcal{G}_c$ in the $\mathbf{x}_u(\mathbf{x}^c)$, $\mathbf{x}_v(\mathbf{x}^c)$, and $\mathbf{x}_t(\mathbf{x}^c)$ directions are equal to the numbers of nodes of $\bar{\mathcal{G}}_c$ in the $\mathbf{U}$, $\mathbf{V}$, and $\mathbf{T}$ directions, respectively;
   - the permeabilities $\bar{\varphi}(\mathbf{u})$ attached to the microcells of $\bar{\mathcal{G}}_c$ are transferred to their corresponding microcells in the grid $\mathcal{G}_c$.
7. Apply any relevant upscaling algorithm to convert the permeabilities contained in the grid $\mathcal{G}_c$ into an unique and equivalent permeability tensor P^c assigned to the flow-cell C.

This procedure is relevant because:

- the images of the vectors $\mathbf{x}_u$, $\mathbf{x}_v$, and $\mathbf{x}_t$ in the $\bar{G}$-space are identical to the constant vectors $\mathbf{U}$, $\mathbf{V}$, and $\mathbf{T}$, respectively (see Eqs. (26));
- the sizes $(\sigma_u^c, \sigma_v^c, \sigma_t^c)$ of the cell C are assumed to be small enough to ensure that the vectors $\mathbf{x}_u(\mathbf{x})$, $\mathbf{x}_v(\mathbf{x})$, and $\mathbf{x}_t(\mathbf{x})$ are more or less constant when $\mathbf{x}$ moves in C;
- in the $\bar{G}$-domain, the box $\bar{B}_c$ and thus the grid $\bar{\mathcal{G}}_c$, are not affected by faults or erosion and thus contains only the image of terrains whose permeabilities are "coherent" with those contained within the cell C.

As a consequence, if $\mathbf{x}_u(\mathbf{x})$, $\mathbf{x}_v(\mathbf{x})$, and $\mathbf{x}_t(\mathbf{x})$ can be assumed to be approximately constant within C, the permeability tensor P^c resulting from the above upscaling technique is representative of the average behavior of flow through the flow-cell C. More generally, one can easily transpose the above proposed technique to upscale any kind of property on C.

CONCLUSIONS

In this article, we have proposed a mathematical framework for the transformation of the geological space G into a new space $\bar{G}$ corresponding to the image of the terrains at geological time of deposition. The initial motivation behind this transformation comes from the fact that physical properties of sedimentary terrains inherit from the paleoenvironment at geological time of deposition. For this reason,

we surmise that modeling properties in the $\bar{G}$-space is more relevant than the classical approach which consists in modeling these properties in the G-space directly. This suggests splitting the modeling of the properties of sedimentary terrains into three successive steps:

1. a first step where the geometry of the geological structures, horizons, and faults, is modeled;
2. a second step where the influence of the geometry of the geological structures is removed;
3. a final step where the properties are modeled.

Adopting such "divide and conquer" approach should result in better modeling of the properties of the sedimentary terrains whatever the interpolation method used. As a consequence, the proposed approach appears as a complement to all the present and future geostatistical methods.

The mathematical framework, called GeoChron, introduced in this article also provides solutions to problems as different as determination of strains resulting from tectonic events and upscaling of permeabilities on structured and unstructured grids. This shows that this framework may be useful to solve, in an unified way, complex theoretical and practical problems.

ACKNOWLEDGMENTS

This research work was performed in the frame of the gOcad research project. The companies and universities members of the gOcad consortium are hereby acknowledged. The author expresses special gratitude to Professor A. G. Journel, Stanford University, and J. J. Royer from CNRS for their critical reviewing of early versions of this article. O. Grosse, R. Moyen and R. Cognot from the gOcad research group are acknowledged for having realized the first computer implementation of the GeoChron model. The author also thanks the reviewers for their comments which contributed to improve this article.

REFERENCES

Aziz, K., and Settari, A., 1979, Petroleum reservoir simulation: Elsevier, New York, 476 p.

Cerveny, V., 1985, The application of ray tracing to the numerical modeling of seismic wave fields in complex structures: Geophysical press, London, Part A, p. 1–124

Chiles, J. P., and Delfiner, P., 1999., Geostatistics—Modeling spatial uncertainties (series in Prob. and Stat.): Wiley, New York, 615 p.

Couples, G. D., Lewis, H., and Tanner, P. W. G., 1998, Strain partitioning during flexural slip folding, *in* Coward, M. P., Daltaban, T. S., and Johnson, H., eds., Structural geology in reservoir characterization, Vol. 127: Geological Society of London Special Publication, p. 149–165.

Dahlstrom, C. D. A., 1969, Balanced cross section: Can. J. Earth Sci., v. 6, p. 743–757.

Darman, N. H., Durlovky, L. J., Sorbie, K. S., and Pickup, G. E. 2000, Up-scaling immiscible gas displacements; quantative use of fine grid flow data in grid coarsening schemes: SPE J., Paper # 59452, 9 p.

Deutsch, C. V., and Journel, A. G., 1998, GSLIB, geostatistical software library and user's guide, (2nd edn.): Oxford University Press, New York, 369 p.

DoCarmo, M., 1976, Differential geometry of curves and surfaces: Prentice Hall, Englewood, NJ, 503 p.

Edington, A., 1923, The mathematical theory of relativity: Cambridge University Press, Cambridge, 247 p.

Einstein, A., 1920, Relativity: The special and general theory: Methuen, London, 138 p.

Gautier, Y., Blunt, M. J., and Christie, M. A., 1999, Nested gridding and steamline-based simulation for fast reservoir performance prediction: Society of Petroleum Engineers, Paper # SPE 51931.

Gibbs, A. D., 1983, Balanced cross-section construction from seismic sections in areas of extentional tectonics: J. Struct. Geol. v. 5, p. 153–160.

Goovaerts, P., 1997, Geostatistics for natural resources evaluation: Oxford University Press, New York, 481 p.

Hubral, P., and Krey, T., 1980, Interval velocities from seismic reflection time measurements: Society of Exploration Geophysicists, Tulsa, OK, 203 p.

Journel, A. G., and Huijbregt, C. J., 1978, Mining geostatstics: Academic Press, New York, 600 p.

Magara, K., 1976, Water expulsion from elastic sediments during compaction: Direction and volumes: Am. Assoc. Pet. Geol. Bull. v. 60, p. 543–553.

Mallet, J. L., 1971, Etude numérique de l'équation de la Diffusion: problème direct, problème inverse: Master Thesis disertation, Institut National Polytehnique de Lorraine.

Mallet, J. L., 2002, Geomodeling: Oxford University Press, New York, 600 p.

Matheron, G., 1968, Les Variables Régionalisées et leur Estimation: Masson, Paris, 190 p.

Mortenson, M. E., 1985, Geometric modeling: Wiley, New York, 763 p.

Renard, Ph., and de Marsily, G., 1997, Calculating equivalent permeability: A review: Adv. Water Resour. v. 20, no. 5/6, p. 253–278.

Sedov, L., 1975, Mécanique des milieux continus: Ed. Mir Moscou, 540 p.

Sokolnikoff, I. S., 1956, Mathematical theory of elasticity: McGraw-Hill, New York, 476 p.

Sokolnikoff, I. S., 1964, Tensor analysis: Theory and applications to geometry and mechanics of continua: Wiley, New York, 361 p.

Suppe, J., 1985, Principles of structural geology: Prentice-Hall, Englewood Cliffs, NJ, 537 p.

Thiele, M., Batycky, R., Blunt, M., and Orr, F., 1996, Simulating flow in heterogeneous media using streamtubes and streamlines: SPE Reservoir Eng. v. 10, no. 1, p. 5–12.

Timoshenko, S. P., and Goodier, J. N., 1970, Theory of elasticity: McGraw-Hill, Auckland, 480 p.

Trykozko, A., Zijl, W., and Bossavit, A., 2001, Nodal and mixed finite elements for numerical homogeneization of 3D permeability: Comput. Geosci. v. 5, p. 61–84.

Wen, X. H., Durlofsky, L. J., and Edwards, M. G., 2003, Use of Border Regions for Improved Permeability Upsaling: Math. Geol. v. 35, no. 5, p. 521–547.

Wheeler, H. E., 1958, Time-stratigraphy: Bull. Am. Assoc. Pet. Geol., v. 42, no .5, p. 1047–1063.